0026-895X/06/7006-2116–2126$20.00
MOLECULAR PHARMACOLOGY
Copyright © 2006 The American Society for Pharmacology and Experimental Therapeutics
Mol Pharmacol 70:2116–2126, 2006

Vol. 70, No. 6
27748/3158347
Printed in U.S.A.

Neurotoxicity of Domoic Acid in Cerebellar Granule Neurons in a Genetic Model of Glutathione Deficiency

G. Giordano, C. C. White, L. A. McConnachie, C. Fernandez, T. J. Kavanagh, and L. G. Costa

Department of Environmental and Occupational Health Sciences, University of Washington, Seattle, Washington (G.G., C.C.W., L.A.M., C.F., T.J.K., L.G.C.); and Department of Human Anatomy, Pharmacology, and Forensic Medicine, University of Parma Medical School, Parma, Italy (L.G.C.)

Received June 8, 2006; accepted September 25, 2006

ABSTRACT

This study investigated the role of cellular antioxidant defense mechanisms in modulating the neurotoxicity of domoic acid (DomA), by using cerebellar granule neurons (CGNs) from mice lacking the modifier subunit of glutamate-cysteine ligase (Gclm). Glutamate-cysteine ligase (Glc) catalyzes the first and rate-limiting step in glutathione (GSH) biosynthesis. CGNs from *Gclm* (−/−) mice have very low levels of GSH and are 10-fold more sensitive to DomA-induced toxicity than CGNs from *Gclm* (+/+) mice. GSH ethyl ester decreased, whereas the Gcl inhibitor buthionine sulfoximine increased DomA toxicity. Antagonists of α-amino-3-hydroxy-5-methyl-4-isoxazolepropionic acid/kainate receptors and of *N*-methyl-D-aspartate (NMDA) receptors blocked DomA toxicity, and NMDA receptors were activated by DomA-induced L-glutamate release. The differential susceptibility of CGNs to DomA toxicity was not due to a differential expression of ionotropic glutamate receptors, as evidenced by similar calcium responses and L-glutamate release in the two genotypes. A calcium chelator and several antioxidants antagonized DomA-induced toxicity. DomA caused a rapid decrease in cellular GSH, which preceded toxicity, and the decrease was primarily due to DomA-induced GSH efflux. DomA also caused an increase in oxidative stress as indicated by increases in reactive oxygen species and lipid peroxidation, which was subsequent to GSH efflux. Astrocytes from both genotypes were resistant to DomA toxicity and presented a diminished calcium response to DomA and a lack of DomA-induced L-glutamate release. Because polymorphisms in the *GCLM* gene in humans are associated with low GSH levels, such individuals, as well as others with genetic conditions or environmental exposures that lead to GSH deficiency, may be more susceptible to DomA-induced neurotoxicity.

In 1987 in Canada, more than 200 people became acutely ill after ingesting mussels. The outbreak resulted in 20 hospitalizations and four deaths. Clinical effects observed included gastrointestinal symptoms and memory loss; for this reason, the condition was termed amnesic shellfish poisoning (Jeffery et al., 2004). The causative agent was soon identified as domoic acid (DomA), a neuroexcitatory toxin whose source was traced to a bloom of the diatom *Pseudo-nitzschia* sp. (Perl et al., 1990). Neuropathological studies revealed neuronal necrosis and astrocytosis, predominantly in the hippocampus and the amygdala (Teitelbaum et al., 1990), and the same pattern of neurotoxic damage was also seen in primates, rats, and mice given DomA (Tryphonas et al., 1990; Strain and Tasker, 1991; Scallet et al., 1993; Sobotka et al., 1996). DomA is a structural analog of kainic acid (KA), an excitatory amino acid that exerts its neurotoxicity by activating the AMPA/KA

This study was supported by National Institutes of Health grants ES012762/NSF-OCE-0434087, R01-ES10849, P42-ES04696, T32-ES007032, and P30-ES07033.
Article, publication date, and citation information can be found at http://molpharm.aspetjournals.org.
doi:10.1124/mol.106.027748.

ABBREVIATIONS: DomA, domoic acid; KA, kainic acid; AMPA, α-amino-3-hydroxy-5-methyl-4-isoxazolepropionic acid; ROS, reactive oxygen species; GSH, glutathione; GSHEE, glutathione ethylester; GCLM, glutamate-cysteine ligase modifier subunit; GCLC, glutamate-cysteine ligase catalytic subunit; MK-801, 5*H*-dibenzo[*a*,*d*]cyclohepten-5,10-imine (dizocilpine maleate); SOD, superoxide dismutase; BSO, L-buthionine-(*S*,*R*)-sulfoximine; BHT, butylated hydroxytoluene; PBN, *N*-*t*-butyl-α-phenylnitrone; DMSO, dimethyl sulfoxide; MTT, 3-(4,5-dimethylthiazol-2-yl)-2,5 diphenyltetrazolium bromide; MBB, monobromobimane; NMDA, *N*-methyl-D-aspartate; CNQX, 6-cyano-7-nitroquinoxaline-2,3-dione disodium; NBQX, 2,3-dihydroxy-6-nitro-sulfamoylbenzo (*f*)quinoxaline; TCEP, tris(2-carboxyethyl)-phosphine hydrochloride; ES, embryonic stem; CGN, cerebellar granule neuron; FBS, fetal bovine serum; SSA, 5-sulfosalicylic acid; GSSG, glutathione disulfide; HPLC, high-performance liquid chromatography; BAPTA-AM, 1,2-bis(2-amino-5-methylphenoxy)ethane-*N*,*N*,*N*′,*N*′-tetraacetic acid tetrakis(acetoxymethyl) ester; $DCFH_2$-DA, 2,7′-dichlorofluorescein diacetate; DCF, 2,7′-dichlorofluorescein; AM, acetoxymethyl ester; MDA, malondialdehyde; γ-GT, γ-glutamyltranspeptidase.

subtype of glutamate receptors (Hampson and Manalo, 1998). The pattern of brain damage observed in humans and in animals after exposure to DomA resembles that seen after administration of KA (Teitelbaum et al., 1990), and a comparison of DomA and KA effects in vitro and in vivo confirms that DomA acts via KA receptors and is 3- to 20-fold more potent than KA itself (Stewart et al., 1990).

Evidence accumulated over the past several years indicates that activation of ionotropic glutamate receptors may be an important source of oxidative stress leading to selective neuronal damage (Coyle and Puttfarcken, 1993). Oxidative stress refers to the cytotoxic consequences of reactive oxygen species (ROS), which are generated as by-products of normal and aberrant metabolic processes that use molecular oxygen. The tripeptide glutathione (GSH) is a major player in cellular defense against ROS, because it nonenzymatically scavenges both singlet oxygen and hydroxyl radicals and is used by glutathione peroxidase and glutathione transferase to limit the levels of certain reactive aldehydes and peroxides within the cell. When ROS production exceeds the antioxidant defense capacity of the cell, oxidative stress ensues, leading to damage of DNA, proteins, and membrane lipids.

In vivo and in vitro studies suggest that oxidative stress is involved in KA neurotoxicity. In rat cortex, KA was found to increase levels of ROS (Bondy and Lee, 1993). In cultured rat retinal neurons, KA produces free radicals (Dutrait et al., 1995), whereas in rat cerebellar granule cells, KA was shown to induce ROS formation and lipid peroxidation (Puttfarcken et al., 1993). Activation of KA in cortical neurons results in marked elevation of intracellular calcium, and this in turn causes oxygen radical production (Carriedo et al., 1998). Administration of KA to gerbils increases free radical formation and lipid peroxidation in the brain (Sun et al., 1992), whereas in rats KA increases mitochondrial superoxide production in the hippocampus (Liang et al., 2000). Various antioxidants have been shown to inhibit KA-induced increases in oxidative stress and neurotoxicity, both in vitro and in vivo (Miyamoto and Coyle, 1990; Puttfarcken et al., 1993; Cheng and Sun, 1994; Wang et al., 2003). Exposure of rat cerebellar granule cells to KA also causes a significant reduction of GSH levels, and addition of GSH ethylester (GSHEE) increases cellular GSH levels, quenches generation of ROS, and reduces the neurotoxicity of KA (Ceccon et al., 2000).

There is only limited information on a possible role of oxidative stress in the neurotoxicity of DomA. In rat cortex, DomA was found to increase levels of ROS (Bondy and Lee, 1993), and DomA-induced neuronal death was attenuated by the centrally acting antioxidant melatonin (Ananth et al., 2003). DomA has also been found to elevate cerebral levels of superoxide dismutase as a consequence to its ability to promote oxidative stress (Bose et al., 1992).

Given the paucity of available information, the present study was undertaken to characterize the role of oxidative stress and of cellular antioxidant defense mechanisms, in DomA-induced neurotoxicity. For this purpose, we used primary cerebellar neurons from *Gclm* (−/−) mice, which lack the modifier subunit of glutamate-cysteine ligase, the first and rate-limiting step in the synthesis of GSH (Yang et al., 2002). In the absence of GCLM, the ability of glutamate-cysteine ligase catalytic subunit (GCLC) to synthesize GSH is drastically reduced (Dalton et al., 2004). Indeed, GSH levels in liver, kidney, pancreas, erythrocytes, and plasma of *Gclm* (−/−) mice are only 9 to 16% of those found in *Gclm* (+/+) animals (Yang et al., 2002). Furthermore, genetic polymorphisms in the human *GCLM* gene have been reported. In particular, a C588T polymorphism in the 5′-flanking region of the gene has been shown to be associated with low plasma levels of GSH (Nakamura et al., 2002). Thus, *Gclm* (−/−) mice may represent a useful model for investigating the effects of compromised GSH synthesis, as has been observed in humans having this polymorphism in *GCLM*.

Materials and Methods

Materials. Neurobasal-A medium, fetal bovine serum (FBS), B27 Minus AO, Hanks' balanced salt solution, GlutaMAX, dispase, and gentamicin were from Invitrogen (Carlsbad, CA). Domoic acid, poly-D-lysine, cytosine β-D-arabinofuranoside, MK-801, superoxide dismutase (SOD), L-buthionine-*(S,R)*-sulfoximine (BSO), butylated hydroxytoluene (BHT), horseradish peroxidase-conjugated anti-mouse IgG, mouse anti-β-actin antibody, horseradish peroxidase-conjugated anti-rabbit IgG, *N*-ethylmorpholine, dimethyl sulfoxide (DMSO), and 3-(4,5-dimethylthiazol-2-yl)-2,5 diphenyltetrazolium bromide (MTT) were from Sigma-Aldrich (St. Louis, MO). Monobromobimane (MBB) was from Chemicon International (Temecula, CA). Protease inhibitors were from Roche Diagnostics (Indianapolis, IN). 6-Cyano-7-nitroquinoxaline-2,3-dione disodium (CNQX), 2,3-dihydroxy-6-nitro-sulfamoylbenzo(*f*)quinoxaline (NBQX), and melatonin were from Tocris Cookson Inc. (Ellisville, MO). The reagents for enhanced chemiluminescence were from GE Healthcare (Little Chalfont, Buckinghamshire, UK). The dNTPs were from Roche Diagnostics, whereas the *Taq* polymerase was from QIAGEN (Valencia, CA). Naphthalene dicarboxaldehyde and 2,7′-dichlorofluorescein diacetate were from Invitrogen. Tris(2-carboxyethyl)-phosphine hydrochloride (TCEP) was from Pierce Chemical (Rockford, IL). The C18 solid phase extraction column was from J. T. Baker (Phillipsburg, NJ).

Generation of *Gclm*-Null Mice and Genotyping. All procedures for animal use were in accordance with the National Institutes of Health Guide for the Use and Care of Laboratory Animals and were approved by the University of Washington Animal Care and Use Committee. *Gclm*-null [*Gclm* (−/−)] mice were derived by homologous recombination techniques in mouse embryonic stem (ES) cells. The β-galactosidase/neomycin phosphotransferase β-Geo fusion gene, a gift from Dr. Phil Soriano (Fred Hutchinson Cancer Research Center, Seattle, WA), was flanked with approximately 2 kilobases of the mouse *Gclm* gene promoter (left arm) and 1.5 kilobases of the first intron (right arm). This construct also contained a diphtheria toxin gene driven by a thymidine kinase promoter to select against random integrants. After selection of transfected 129SV strain ES cells with G418 (Geneticin; Invitrogen), surviving colonies were assessed for targeted integration (disruption of the first exon with β-Geo) using polymerase chain reaction. ES cells with the proper polymerase chain reaction product length were then assessed by restriction digestion and Southern blot analyses. ES cells from correctly targeted clones were subsequently injected into C57BL/6 mouse blastocysts and transplanted into pseudopregnant mice according to standard techniques. Chimeric male pups born from these mothers were mated to C57BL/6 females. Black agouti offspring were screened for the targeted allele. These heterozygotes were intercrossed to obtain *Gclm* (−/−) mice. Upon generation of the *Gclm* (−/−) mice, they were then crossed onto a C57BL/6 background for at least seven generations before experiments. To genotype pups, we analyzed for the presence of both the native *Gclm* gene and β-Geo sequences in two separate reaction mixtures. The reactions used the same *Gclm* upstream primer 5′-GCC CGC TCG CCA TCT CTC-3′ (1 nM), whereas the β-Geo sequence was detected with the reverse primer 5′-CAG TTT GAG GGG ACG ACG ACA-3′ (1.25 nM), and the native *Gclm* sequence was detected with the reverse primer 5′-GTT

GAG CAG GTT CCC GGT CT-3′ (0.5 nM). Reactions (20 μl total volume) contained 0.4 mM each dNTP, 1 unit of *Taq* polymerase, 1× reaction buffer, and 0.8 M DMSO. The cycling conditions were as follows: 94°C for 2 min, followed by 35 cycles of 94°C for 45 s, 60°C for 45 s, and 72°C for 2 min, and a final extension at 72°C for 5 min. Amplicons were resolved by agarose gel electrophoresis and stained with ethidium bromide. Of all mice genotyped, 28% were *Gclm* (+/+), 46% were *Gclm* (+/−), and 26% were *Gclm* (−/−); these numbers approximate the expected Mendelian percentages of 25:50:25 and indicate that no embryonic lethality occurred as a result of the *Gclm* targeting.

Cultures of Cerebellar Granule Neurons. Cultures of cerebellar granule neurons (CGNs) were prepared from 7-day-old mice sacrificed by decapitation. Cerebella were rapidly dissected from the brain in Hibernate A/B27 (Invitrogen) meninges were removed, and tissue was cut into 2-mm cubes. The tissue matrix was loosened by treating with Hibernate A containing 3 mg/ml dispase for 30 min at 37°C. The tissue pieces were allowed to settle for 5 min, and the pellet was resuspended in Hibernate A medium containing 10% FBS and 0.01 mg/ml DNase, before being mechanically dissociated by trituration using a long-stem Pasteur pipette. After dissociation the cell suspension was centrifuged in a refrigerated centrifuge at 300*g* for 5 min. The cell pellet was resuspended in complete growth medium consisting of Neurobasal A medium containing 1 mM GlutaMAX, 100 U/ml penicillin, 100 mg/ml streptomycin, and 10% FBS. A 50-μl sample of resuspended cells was added to a same volume of solution of trypan blue (0.04% in phosphate-buffered saline) and the percentage of viable cells was determined in a hemacytometer. To remove any glial cells, the cell suspension was preplated for 20 min. After two preplating steps, a higher than 97 to 98% purity of granule cells was achieved according to immunocytochemical criteria. The cells were seeded at a density of 1×10^6 cells/cm^2 in Neurobasal A with 10% FBS in humidified 95% air, 5% CO_2 at 37°C. After 24 h, the medium was removed and substituted with fresh prewarmed Neurobasal A containing B27 Minus AO. This medium supplement (B27 Minus AO) is a newly improved formulation without antioxidants and provides a sensitive and powerful antioxidant-free primary culture system.

Cultures of Cerebellar Astrocytes. Cerebellar astrocytes obtained from brains of 7- to 8-day-old mice were prepared according to a method described previously (Guizzetti et al., 2003) with minor modifications. Cells were grown in Dulbecco's modified Eagle's medium supplemented with 10% fetal bovine serum, penicillin, and streptomycin in humidified 95% air, 5% CO_2 at 37°C. After 1 week, cells were dissociated with 0.25% trypsin and 0.1% DNase in Hanks' balanced salt solution and subcultured in six- or 24-well multiplates. Culture medium was changed twice weekly. Cultures contained more than 95% astrocytes as assessed by immunostaining for glial fibrillary acidic protein.

Immunoblotting Analyses. Neurons were scraped in lysis buffer (Tris 50 mM, pH 7.5, 2 mM EDTA, 0.5 mM EGTA, 0.5 mM phenylmethylsulfonyl fluoride, 0.5 mM dithiothreitol, 10 μg/ml leupeptin, 2 μg/ml aprotinin, 1 mM sodium orthovanadate, 1 mM NaF, and 0.25% SDS). Whole homogenates were subjected to SDS-polyacrylamide gel electrophoresis and immunoblotting as described previously (Giordano et al., 2005), using rabbit antibodies against Gclc or Gclm proteins (both diluted 1:1500) or mouse anti-β-actin antibody (1:5000). After electrophoresis, proteins were transferred to polyvinylidene difluoride membranes that were incubated with the above-mentioned antibodies. Membranes were rinsed in Tris-buffered saline and incubated with horseradish peroxidase-conjugated anti-rabbit IgG for GCLC and GCLM, or with horseradish peroxidase-conjugated anti-mouse IgG for actin at the appropriate dilutions (1:5000 for anti-Gclm and Gclc and 1:15,000 for anti-actin antibodies).

Measurement of GSH Levels. Total intracellular GSH levels were measured using the following procedure. Neurons were homogenized in Locke's buffer and an aliquot was taken to measure the protein concentration, whereas a second aliquot was diluted (1:1) in 10% 5-sulfosalicylic acid (SSA). The SSA fraction was centrifuged at 12,000 rpm for 5 min at 4°C, and the supernatant was used for GSH determinations. Aliquots from the SSA fraction were added to a black flat-bottomed 96-well plate, and pH was adjusted to 7 with 0.2 M *N*-ethylmorpholine/0.02 M KOH. Oxidized glutathione was reduced by adding 10 μl of 10 mM TCEP for 15 min at room temperature. The pH was then adjusted to 12.5 by using 0.5 N NaOH before derivatizing the samples with 10 mM naphthalene dicarboxaldehyde for 30 min. Finally, the samples were analyzed on a spectrofluorometric plate reader (λ_{EX} = 472 and λ_{EM} = 528 nm). After incubation, the total amount of GSH in the sample was expressed as nanomoles per milligram of protein determined from a standard curve obtained by plotting known amounts of GSH incubated in the same experimental conditions versus fluorescence.

Measurement of Intracellular GSSG/GSH Ratio. Intracellular glutathione disulfide (GSSG)/GSH ratio was assayed using MBB as reported previously (Thompson et al., 2000) with modifications as follows. In brief, cells were collected and washed in 1 ml of Locke's buffer, pH 7.4, and centrifuged for 5 min at 300*g*. The supernatant was discarded, and the cell pellet was resuspended in 150 μl of Locke's buffer. An aliquot of 50 μl was taken to measure the protein level and to determine cell viability (by trypan blue exclusion), whereas a second aliquot was diluted (1:1) with 10% SSA to avoid oxidation of GSH and to induce cell lysis. Two aliquots containing the same amount of protein were taken from each sample; one aliquot was reduced via addition of 10 μl of 10 mM TCEP to determine total glutathione, whereas to the second aliquot a volume of 10 μl of water was added for 15 min at 4°C to determine reduced glutathione. A volume of 20 μl of 12.5 mM MBB solution was added for 30 min. GSSG was calculated by subtracting reduced GSH from total glutathione. To ensure that TCEP effectively reduced all of the GSSG in the sample to GSH, known amounts of GSSG were added to the extract and incubated in presence of TCEP. HPLC analysis indicated that other compounds present in the extract did not consume TCEP and that the levels of GSSG in control samples were approximately 3% of total intracellular glutathione. The values for GSH and GSSG were calculated from the mean of triplicate runs for each sample. The coefficient of variation for measurements of GSH and GSSG were 3.9 and 17.8%, respectively.

Measurement of GSH Efflux. GSH efflux from neurons was measured using a modification of White et al. (1999). Samples of Locke's buffer (5 ml) from treated and untreated CGNs were reduced with 20 μl of 10 mM TCEP for 20 min at room temperature and then derivatized with 20 μl of 2.5 mM MBB solution for 30 min in the dark. The pH was then adjusted to 2.0 by adding 1 ml of 5% SSA. The samples were then concentrated on a C18 solid phase extraction column using a vacuum manifold. MBB-glutathione conjugate was eluted from the column with 1 ml of ice-cold methanol. Finally, 25 μl of the eluate was analyzed by HPLC against known standards.

Cytotoxicity Assay. DomA, GSH ethyl ester, NBQX, CNQX, MK-801, BAPTA-AM, and SOD were dissolved in Locke's solution, whereas BHT and *N*-*t*-butyl-α-phenylnitrone (PBN) were dissolved in DMSO. Cells were washed once with Locke's solution, and DomA was added for 1 h, whereas antioxidants or receptor antagonists were added 30 min before the DomA treatment. At the end of DomA exposure, cultures were washed twice with Locke's solution and returned to their culture-conditioned medium for a further 24 h. Cell survival was quantified by a colorimetric method using the metabolic dye MTT. Culture medium was removed and replaced with 500 μl/well of Locke's solution containing 2 mg/ml MTT. After incubation for 30 min at 37°C, the MTT solution was removed, and the formazan reaction product was dissolved in 250 μl of DMSO. Absorbance was read at 570 nm, and the results expressed as percentage of viable cells relative to unexposed controls.

Assay of Reactive Oxygen Species Formation. ROS formation was determined by fluorescence using 2,7′-dichlorofluorescein diacetate ($DCFH_2$-DA). $DCFH_2$-DA is readily taken up by cells and is

subsequently de-esterified to $DCFH_2$ (relatively low fluorescence). $DCFH_2$ can be oxidized to dichlorofluorescein (DCF) by hydrogen peroxide, peroxynitrite, and other ROS/reactive nitrogen species (Oyama et al., 1994; Kooy et al., 1997). In a typical experiment, cells were first washed with Locke's solution and then preincubated for 30 min at 37°C with $DCFH_2$-DA (50 nmol/mg of cell protein) in Locke's solution. $DCFH_2$-DA was added from a stock solution in methanol. Cells were then washed with Locke's solution to remove extracellular $DCFH_2$-DA. After treatments (at 37°C), the incubation solution was removed, and 0.1 M KH_2PO_4 and 0.5% Triton X-100, pH 7.2, was added for 10 min. Cell lysates were then scraped from the dish, and the extract was centrifuged for 10 min at 12,000 rpm. The supernatant was collected, and the fluorescence was immediately read using a spectrofluorimeter (excitation, 488 nm; emission, 525 nm; PerkinElmer Life and Analytical Sciences, Boston, MA). ROS formation was expressed as the amount of DCF formed using a DCF standard curve (0.01–100 μM).

Fluorescence Imaging of Cytoplasmic Free Ca^{2+} in Single Cells. CGNs or astrocytes were loaded with the Ca^{2+}-sensitive fluorescent dye fluo-3/AM (3 μM for neurons and 10 μM for astrocytes) at 37°C for 60 min in culture medium. Cells were then washed and incubated for an additional 30 min in a fluo-3/AM-free Locke's buffer to remove extracellular traces of the dye and to complete intracellular de-esterification. The 35-mm plates were placed on the stage of an inverted microscope. In some cases, a Ca^{2+}-free condition was achieved in Ca^{2+}-free Locke's buffer containing 0.1 mM EGTA. The dye in the cytoplasmic portion of the cells was excited, and fluorescence images were captured at 20-s intervals by a MicroMax cooled charge-coupled device camera (Princeton Instruments, Trenton, NJ) using MetaMorph software (Molecular Devices, Sunnyvale, CA).

Measurement of Lipid Peroxidation. CGNs were scraped in 20 mM phosphate buffer, pH 7.4, and aliquots were removed to determine the protein content. After addition of an antioxidant (10 μM BHT) to prevent sample oxidation, the homogenate was centrifuged at 3000*g* for 10 min to remove large cell fragments. *N*-Methyl-2-phenylindole and methanesulfonic acid were then added, and the samples were incubated at 45°C for 60 min and then centrifuged at 5000*g* for 10 min to obtain a clear supernatant. Absorbance of the supernatant was read at 586 nm. Preliminary experiments designed to characterize the assays used in the our study found that samples containing the growth medium without cerebellar granule cells produced a significant absorbance reading for the ROS and lipid peroxidation assays. These false signals are most likely due to various components such as trace metals. For this reason, these experiments were performed in Locke's solution.

Measurement of L-Glutamate Release. Exposure conditions in L-glutamate release studies were identical to those used in the excitotoxicity assay. Buffers from treated cells were collected, and determination of L-glutamate was carried out using the GLN-kit (Sigma-Aldrich). This kit is designed for the spectrophotometric measurement of L-glutamine and/or L-glutamate via enzymatic deamination of L-glutamine and dehydrogenation of L-glutamate with reduction of NAD^+ to NADH. The conversion of NAD^+ to NADH was measured spectrophotometrically at 340 nm and is proportional to the amount of glutamate that is oxidized.

Statistical Analysis. Data are expressed as the mean ± S.D. of at least three independent experiments. Statistical analysis was performed by Student's *t* test for paired samples or by one-way analysis of variance followed by a Bonferroni post test.

Results

GSH Levels in Cultured Neurons and Astrocytes from *Gclm* (−/−), *Gclm* (+/−), and *Gclm* (+/+) Mice. As expected, the Gclm protein is not present in CGNs from *Gclm* (−/−) mice, whereas the Gclc protein level is increased (Fig. 1A). Gclm is known to bind to Gclc and change the catalytic characteristics of Gclc in vitro. Because Gclc alone [in a *Gclm* (−/−) mouse] is predicted to function poorly in synthesizing γ-glutamylcysteine, the very low levels of GSH found in both CGNs and cerebellar astrocytes from *Gclm* (−/−) mice (Fig. 1B) is not surprising. Cells from *Gclm* (+/−) mice displayed GSH levels similar to those found in *Gclm* (+/+) mice (Fig. 1B). The higher GSH levels found in cerebellar astrocytes compared with CGNs are in agreement with a previous study (Huang and Philbert, 1995). Of note is that CGNs, in contrast to other neuronal cell types, contain relatively high levels of GSH (Lowndes et al., 1994). Intracellular GSH content of CGNs declined as a function of culture age (20–25% at day in vitro 12), in contrast to cerebellar astrocytes where it was constant with time (data not shown).

***Gclm* (−/−) Cerebellar Granule Neurons Are More Sensitive Than *Gclm* (+/+) Cells to DomA-Induced Neurotoxicity.** To test the hypothesis that CGNs from *Gclm* (−/−) mice might be more sensitive to DomA-induced toxicity, cell viability was measured by the MTT reduction assay. The IC_{50} values for DomA were 3.4 ± 1.3 μM in *Gclm* (+/+) neurons and 0.39 ± 0.3 μM in *Gclm* (−/−) neurons ($p < 0.01$). These experiments as well as those that followed were also carried out in CGNs from *Gclm* (+/−) mice. Because no significant differences were found between *Gclm* (+/+) and *Gclm* (+/−) neurons in response to DomA [IC_{50} of DomA was 3.1 ± 1.1 μM for *Gclm* (+/−) neurons], results obtained in *Gclm* (+/−) cells are not shown. DomA did not cause any loss

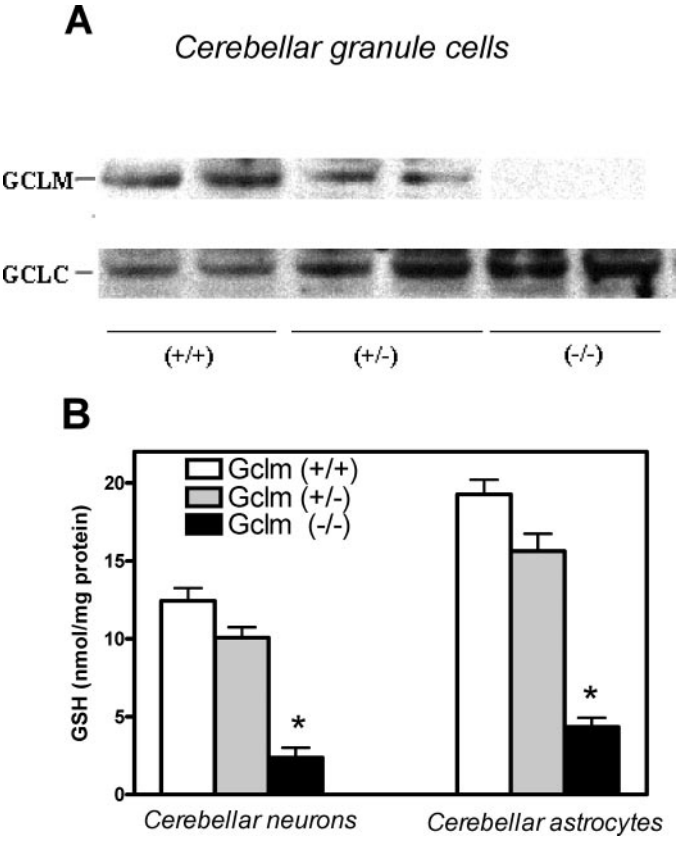

Fig. 1. A, Western blot analysis of Gclm and Gclc proteins in mouse CGNs. B, GSH levels in CGNs and cerebellar astrocytes from *Gclm* (+/+), *Gclm* (+/−), and *Gclm* (−/−) mice. Results represent the mean ± S.D. of at least three experiments. ∗, significantly different from *Gclm* (+/+) ($p < 0.01$).

of viability in cerebellar astrocytes (Fig. 2B), irrespective of genotype.

The differential toxicity of DomA in CGNs from *Gclm* (+/+) and *Gclm* (−/−) mice was not due to a different expression of ionotropic glutamate receptors, as evidenced by a similar calcium response evoked by DomA in both cell types (Fig. 2C). In contrast, the calcium response induced by DomA in cerebellar astrocytes was much smaller (Fig. 2C). In CGNs, calcium increase evoked by DomA was antagonized by the kainate/AMPA receptor antagonist NBQX and by the NMDA receptor antagonist MK-801, whereas in astrocytes only NBQX was effective (Fig. 2D).

To investigate the role of GSH in the neurotoxicity of DomA, CGNs were incubated with the GSH delivery agent GSHEE (2.5 mM). This treatment significantly increased cellular GSH content by 30 min (Fig. 3A) and prevented the toxicity of DomA (Fig. 3B). Furthermore, when CGNs from *Gclm* (+/+) mice were exposed to BSO (an irreversible inhibitor of Gcl) at 25 μM for 24 h, the expected depletion of intracellular GSH occurred [from 12.43 ± 1.4 to 3.7 ± 2.1 nmol/mg of protein, an amount roughly equivalent to that in *Gclm* (−/−) cells], and the toxicity of DomA was significantly increased (Fig. 3C). Note that under these conditions, *Gclm* (+/+) neurons are as sensitive to DomA as *Gclm* (−/−) cells (not treated with BSO).

Pharmacological Analysis of DomA Toxicity. To investigate the role of ionotropic glutamate receptors in DomA-induced cytotoxicity, *Gclm* (+/+) and *Gclm* (−/−) neurons were preincubated with different antagonists. In the presence of 10 μM NBQX, a concentration that would prevent the activation of AMPA and KA receptors (Sheardown et al., 1990), DomA-induced toxicity was completely blocked (Fig. 4). Similar results were found with another AMPA/KA receptor antagonist, CNQX (10 μM), and with the NMDA receptor antagonist MK-801, indicating that DomA toxicity is mediated by both AMPA/KA and NMDA receptors in mouse CGNs (Fig. 4). Furthermore, the calcium chelator BAPTA-AM also prevented DomA-induced toxicity (Fig. 4). To test the hypothesis that NMDA receptors may be activated as a consequence of DomA-stimulated release of endogenous L-glutamate,

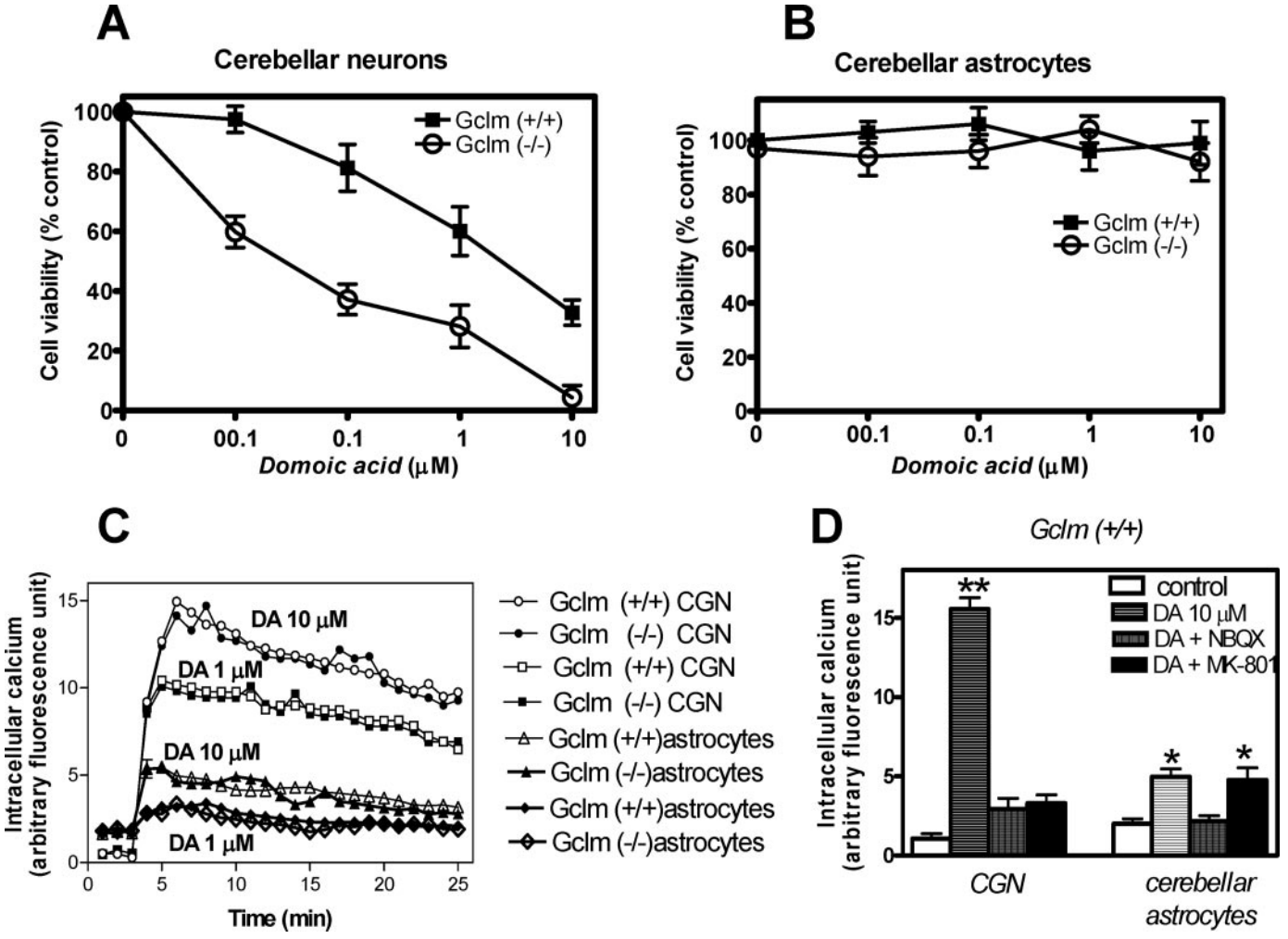

Fig. 2. Effect of DomA on viability and calcium response in CGNs and cerebellar astrocytes. CGNs (A) and cerebellar astrocytes (B) from mice of both *Gclm* (+/+) and (−/−) genotypes were treated with DomA, and cell viability was assessed after 24 h by MTT reduction. Data are presented as percentage of untreated CGNs taken as control and represent the mean ± S.D. of at least three experiments. All points in *Gclm* (−/−) CGNs are significantly different from *Gclm* (+/+) CGNs ($p < 0.01$). In C, the effects of 1 and 10 μM DomA on $[Ca^{2+}]_i$ levels in CGNs and astrocytes of both *Gclm* (+/+) and (−/−) genotypes, as measured by fluo-3 fluorescence, are shown. The effects of 10 μM NBQX and 5 μM MK-801 on $[Ca^{2+}]_i$ increase induced by 10 μM DomA in CGNs and cerebellar astrocytes from *Gclm* (+/+) mice are shown in D. Data are expressed as arbitrary units of fluorescence and represent the mean ± S.D. of three experiments. *, significantly different from control astrocytes ($p < 0.05$). **, significantly different from control CGNs ($p < 0.01$).

CGNs were exposed to 10 μM DomA for 10 min, and the incubation buffers were assayed for the presence of L-glutamate. Results of L-glutamate measurements were normalized to total protein content to account for variations in the numbers of cells on the plate. Figure 5 shows the efflux of L-glutamate after a 15-min DomA exposure in CGNs (A) and cerebellar astrocytes (B). In CGNs, DomA increased L-glutamate release. This was completely prevented by NBQX and attenuated by BAPTA-AM and MK-801. This suggests that DomA, through activation of non-NMDA receptors, induces the release of L-glutamate from CGNs, and this L-glutamate, in turn, activates NMDA receptors, which promote further increases in L-glutamate efflux (Berman and Murray, 1997). In contrast, DomA did not cause any release of L-glutamate from cerebellar astrocytes (Fig. 5B).

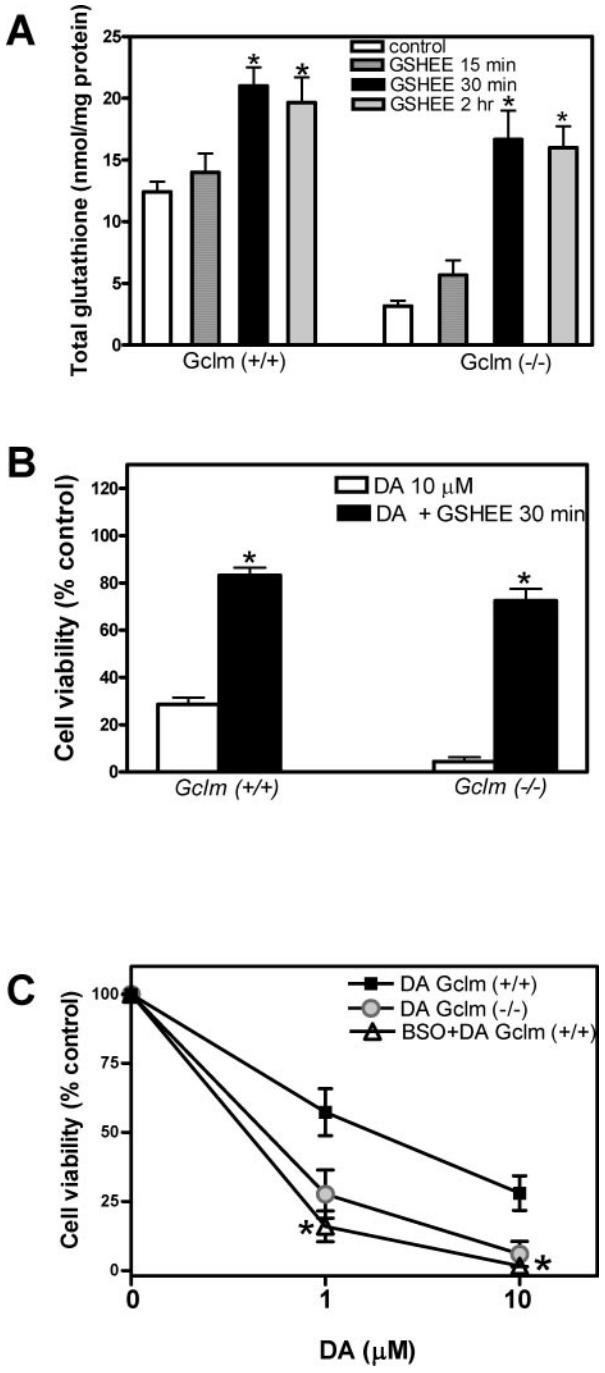

Fig. 3. A, total GSH levels in *Gclm* (+/+) and *Gclm* (−/−) CGNs after exposure to 2.5 mM GSHEE for different times. Data are expressed as nanomoles of glutathione per milligram of protein and represent the mean ± S.D. of at least three experiments. ∗, significantly different from control ($p < 0.01$). B, toxicity of 10 μM DomA after a 30-min pretreatment with 2.5 mM GSHEE, as assessed by the MTT reduction assay. Data represent the mean ± S.D. of at least three experiments. ∗, significantly different from DomA-treated cells of the same genotype ($p < 0.01$). C, effect of BSO pretreatment on DomA-induced toxicity. CGNs from *Gclm* (+/+) mice were pretreated with 25 μM BSO for 24 h and then challenged with 10 μM DomA. ∗, significantly different from *Gclm* (+/+) CGNs in the absence of BSO ($p < 0.05$). Data represent the mean ± S.D. of at least three experiments.

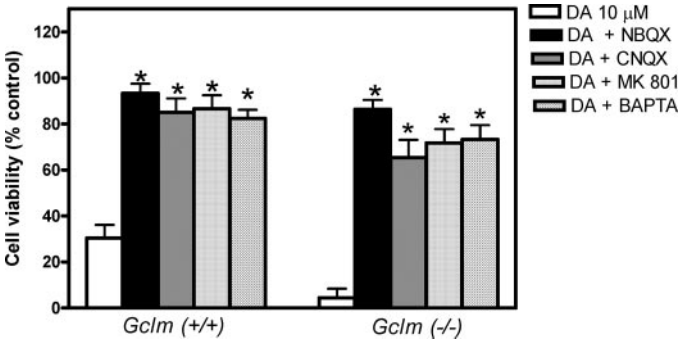

Fig. 4. Effects of 10 μM NBQX, 50 μM CNQX, 5 μM MK-801, and 5 μM BAPTA-AM on 10 μM DomA-induced toxicity in CGNs. Results are expressed as percentage of untreated CGNs and represent the mean ± S.D. of at least three experiments.∗, significantly different from DomA-treated CGNs ($p < 0.01$).

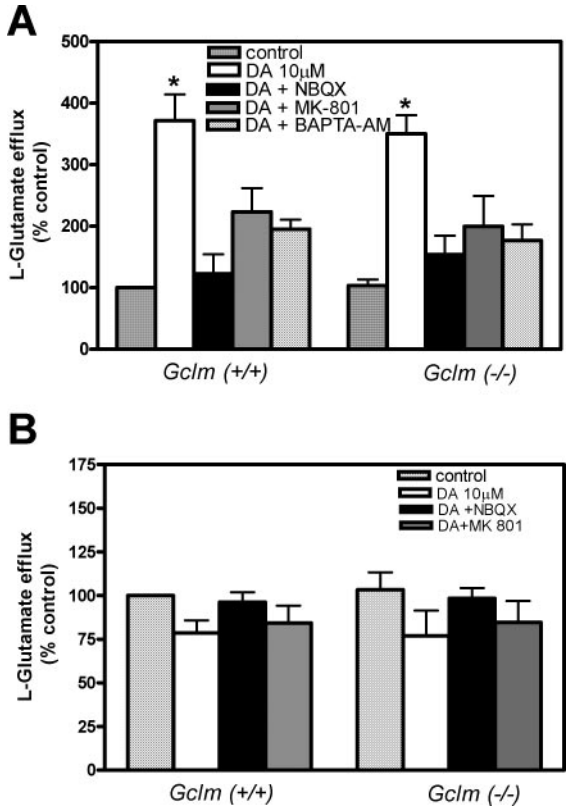

Fig. 5. Efflux of L-glutamate from CGNs (A) and cerebellar astrocytes (B) exposed to 10 μM DomA for 15 min or DomA in combination with either 10 μM NBQX, 5 μM MK-801, or 5 μM BAPTA-AM. Results are expressed as percentage of control for each genotype. Data represent the mean ± S.D. of at least three experiments. ∗, significantly different from control ($p < 0.01$).

Antioxidants Prevent DomA Toxicity. To further investigate the role of oxidative stress in DomA-induced neurotoxicity, CGNs were preincubated with antioxidants PBN (100 μM), SOD (100 U/ml), melatonin (200 μM), and BHT (100 μM) followed by treatment with DomA. All compounds protected *Gclm* (+/+) and *Gclm* (−/−) neurons against DomA-induced neurotoxicity (Fig. 6). The free radical spin trapping agent PBN was particularly effective at preventing DomA-induced neurotoxicity, suggesting that the generation of superoxide and free radicals might have a central role in DomA-induced cell death.

Effect of DomA on ROS Production and Lipid Peroxidation. ROS production was measured with the oxidant-sensitive fluorescent dye $DCFH_2$-DA. DomA caused a significant time- and concentration-dependent increase in ROS production, with a maximal effect after 1-h incubation (Fig. 7, A and B). Production of ROS was significantly higher in *Gclm* (−/−) neurons (21.97 ± 1.26 pmol DCF/mg of protein) than in *Gclm* (+/+) neurons (10.23 ± 1.05 pmol DCF/mg of protein) ($p < 0.01$). The AMPA/KA receptor antagonists NBQX and CNQX, the NMDA receptor antagonist MK-801, and BAPTA-AM significantly attenuated the ROS production induced by DomA (Fig. 7C). Antioxidants and GSHEE also inhibited DomA-induced ROS formation (Fig. 7D). Thus, all compounds that inhibit DomA-induced cytotoxicity also reduce DomA-induced production of ROS.

The ability of DomA to induce lipid peroxidation was assessed by determining changes in malondialdehyde (MDA) concentrations. A time-course experiment indicated that the maximum increase in lipid peroxidation was present approximately 2 h after DomA exposure (data not shown). DomA caused an increase in MDA levels, which was significantly greater in CGNs from *Gclm* (−/−) mice (Table 1). DomA-induced lipid peroxidation was inhibited by GSHEE, NBQX, and MK-801 (Table 1).

Effect of DomA on Intracellular Levels of GSH and GSSG and on GSH Efflux. DomA caused a time-dependent loss of total cellular GSH in CGNs (Fig. 8A). This decrease was prevented by ionotropic glutamate receptor antagonists but not by antioxidants (Fig. 8B). Near maximal depletion of cellular GSH was observed after 1-h incubation with DomA, before any cytotoxicity is apparent (Fig. 8C).

Cellular GSH levels are thought to be determined by the rates of synthesis and loss of the tripeptide via oxidation, use in glutathione transferase-mediated conjugation reactions, γ-glutamyltranspeptidase (γ-GT)-mediated amino acid transport, or by excretion. GSH depletion is commonly observed when cells are oxidatively stressed and can be detected by measurement of transient increases in intracellular GSSG content. Despite a massive and rapid GSH loss, there was only a modest increase in GSSG intracellular content upon exposure to DomA, which was prevented by NBQX and MK-801 (Fig. 9A). Declining GSH levels might result either from an increased efflux out of the cell or a reduced rate of synthesis. To discriminate between these two possibilities, GSH synthesis was blocked by BSO; this treatment decreased intracellular GSH levels by approximately 40 to 45% after 6 h (Fig. 9B). However, DomA induced a much more rapid drop in GSH levels (Fig. 9B). To determine whether GSH was being extruded from the CGNs, the incubation medium was collected and derivatized with monobromobimane before analysis by HPLC. DomA caused an increase of net efflux of total GSH in *Gclm* (+/+) and *Gclm* (−/−) neurons, which was prevented by ionotropic glutamate receptor antagonists (Fig. 9C). Because extracellular GSH may be used by γ-GT, the experiments were carried out with 0.2 mM acivicin, an inhibitor of this enzyme. Similar to earlier studies (Wallin et al., 1999), we found that inhibition of γ-GT activity increased the recovery of GSH in the medium. A time-course experiment shows that efflux of glutathione from DomA-treated cells begins after 15 min of DomA treatment (Fig. 9D), concomitant with the decrease in intracellular GSH (Fig. 8A). Efflux of GSH and the decrease in intracellular GSH precede the production of ROS induced by DomA (Fig. 7A).

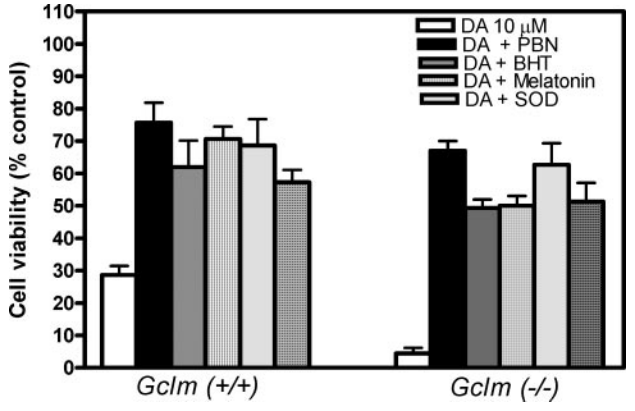

Fig. 6. Antioxidants protect CGNs from DomA-induced neurotoxicity. CGNs of both genotypes were exposed to 10 μM DomA, alone or in combination with 100 μM PBN, 100 U/ml SOD, 200 μM melatonin, or 100 μM BHT at 37°C for 60 min. Cell survival was quantified 24 h later by the MTT assay. The protection afforded by all antioxidants in preventing DomA-induced toxicity was statistically significant in both genotypes ($p < 0.01$). Data represent the mean ± S.D. of at least three experiments.

Discussion

Although DomA is a well known neurotoxin, the biochemical mechanisms involved in its neurotoxic effect are still elusive. Because of its structural similarity to KA, DomA is thought to exert its neurotoxicity by binding to and activating a subclass of non-NMDA excitatory amino acid receptors, the AMPA/KA receptors.

KA neurotoxicity has been suggested to be mediated by increased oxidative stress (Sun et al., 1992; Bondy and Lee, 1993; Puttfarcken et al., 1993; Carriedo et al., 1998; Liang et al., 2000). In this study, we investigated the role of GSH in modulating the toxicity of DomA. For this purpose, we used a genetic model of GSH deficiency (i.e., CGNs derived from mice with compromised GSH synthesis) because of the lack of the modifier subunit of glutamate-cysteine ligase [*Gclm* −/− mice]. Our results indicate that GSH plays a critical role in modulating the neurotoxicity of DomA, and this is supported by various lines of evidence. First, *Gclm* (−/−) neurons, which have a much lower levels of GSH, are 10-fold more sensitive to DomA toxicity than CGNs from *Gclm* (+/+) mice. Second, the membrane-permeant GSH delivery agent GSHEE restored intracellular GSH levels in *Gclm* (−/−) neurons, and this afforded protection against DomA-induced toxicity. Third, depletion of GSH by L-buthionine sulfoximine in *Gclm* (+/+) CGNs rendered them as sensitive to DomA as

Gclm (−/−) neurons. The different susceptibility of CGNs from the two mouse strains was not due to different expression of ionotropic glutamate receptors, as suggested by the fact that DomA induced an identical calcium response in both *Gclm* (+/+) and *Gclm* (−/−) neurons.

Neurotoxicity of DomA was antagonized by AMPA/KA receptor antagonists and by an antagonist of NMDA receptors. The involvement of NMDA receptors is most likely due to DomA-induced release of L-glutamate, as suggested previously (Berman and Murray, 1997; Berman et al., 2002). The finding that MK-801 inhibited DomA-induced L-glutamate release suggests that activation of NMDA receptors by the released L-glutamate further promotes L-glutamate release. It should be noted that DomA-induced L-glutamate release was similar in *Gclm* (+/+) and (−/−) neurons, indicating that this process does not explain their differential susceptibility to DomA toxicity.

DomA-induced neurotoxicity was also prevented by several antioxidants, in both *Gclm* (+/+) and (−/−) neurons. A particularly effective antioxidant was the free radicals spin trapping agent PBN, suggesting that superoxide and free radical may be generated by DomA in CGNs. Indeed, DomA caused a time- and concentration dependent increase in ROS, which was significantly higher in CGNs from *Gclm* (−/−) mice. Such DomA-induced increases in ROS were antagonized by AMPA/KA and NMDA receptor antagonists, by GSH ethyl ester, and by antioxidants. Because one consequence of increased ROS production is an increase in lipid peroxidation, we determined whether the latter was increased by DomA. This was indeed the case, with a greater increase in MDA production in *Gclm* (−/−) neurons compared with their wild-type counterparts.

To probe the mechanism underlying the increased ROS production induced by DomA, we investigated the effect of DomA on intracellular GSH levels. In both *Gclm* (+/+) and *Gclm* (−/−) neurons, DomA induced a time-dependent decrease of intracellular GSH. This effect was not due to inhibition of GSH synthesis by DomA, as suggested by a compar-

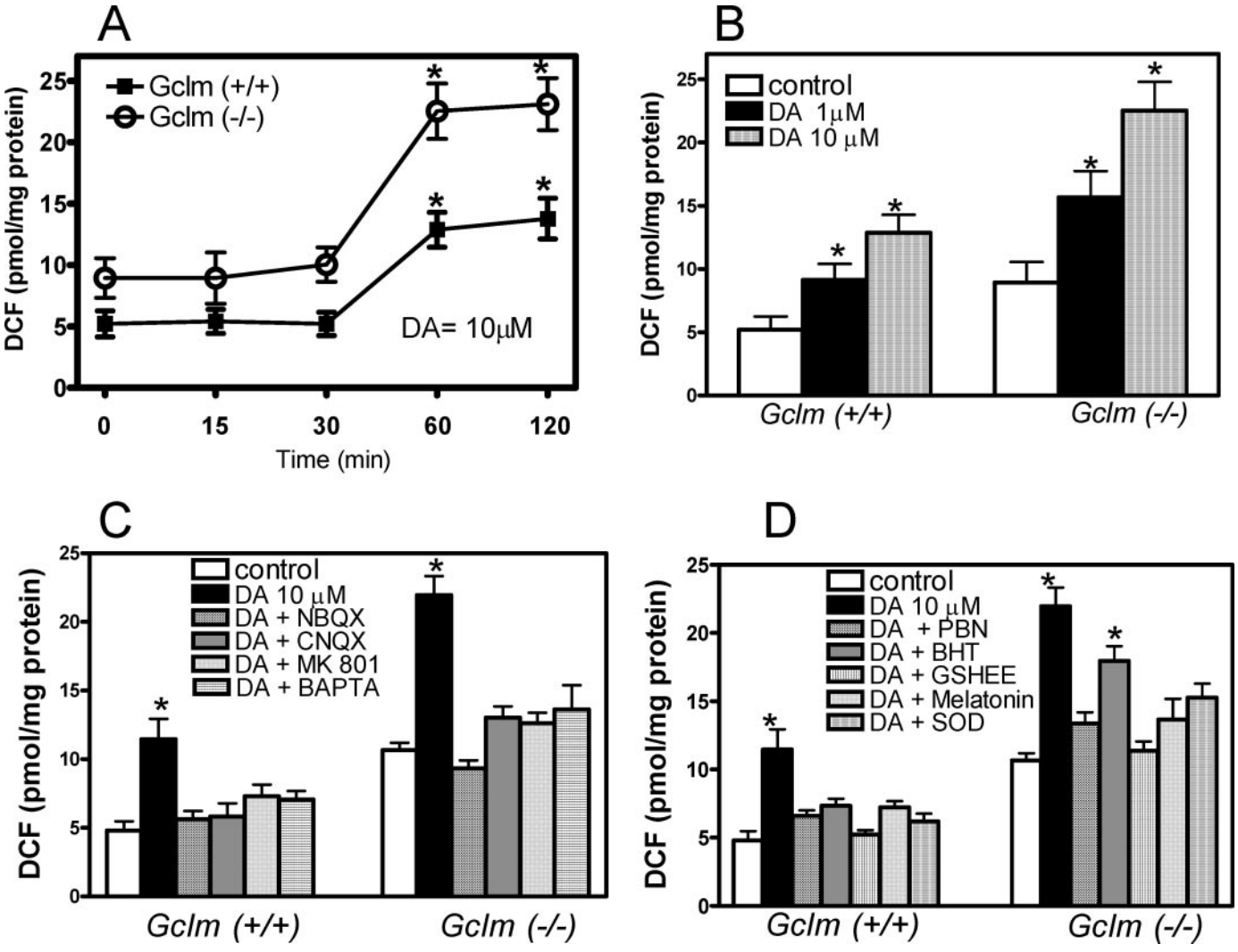

Fig. 7. A, time course of ROS production after treatment with 10 μM DomA. Results represent the mean ± S.D. of at least three experiments. ∗, significantly different from the respective control ($p < 0.05$). B, concentration-response effect of DomA on ROS levels, measured at 60 min. Results represent the mean ± S.D. of at least three experiments. ∗, significantly different from control ($p < 0.05$). C and D, effect of glutamate receptor antagonists (C) and antioxidants (D) on DomA-induced ROS generation in CGNs. Cells of both genotypes were incubated with 10 μM DomA, alone or in combination with either 5 μM MK-801, 10 μM NBQX, 10 μM CNQX, 5 μM BAPTA-AM, 100 μM PBN, 100 U/ml SOD, 200 μM melatonin, or 100 μM BHT. Results represent the mean ± S.D. of at least three experiments. ∗, significantly different from untreated cells of the same genotype ($p < 0.05$).

ison of the time courses of GSH decline upon exposure to DomA and BSO. Alternative explanations for the DomA-induced GSH loss would be oxidation to GSSG or its release from the cell. DomA caused only a modest increase in intracellular GSSG content. However, it caused a highly significant increase in GSH efflux from both *Gclm* (+/+) and *Gclm* (−/−) neurons.

The calcium chelator BAPTA-AM also antagonized DomA-induced toxicity, L-glutamate release, and GSH efflux, suggesting an involvement of calcium in these effects. A comparison of the time course of DomA-induced effects in CGNs suggests the following sequence of events in DomA-mediated neurotoxicity. By activating AMPA/KA receptors, DomA causes an increase in $[Ca^{2+}]_i$, which then results in a release of L-glutamate. This released L-glutamate in turn activates NMDA receptors and promotes further L-glutamate release. This combined action causes a rapid accumulation in $[Ca^{2+}]_i$, promotes GSH efflux, and causes a concomitant decrease in intracellular GSH. High $[Ca^{2+}]_i$ and low intracellular GSH lead to production of ROS, which are probably of mitochondrial origin (Carriedo et al., 1998). Because there is insufficient GSH to scavenge the ROS, there is an increase in lipid peroxidation, and this contributes to cell death. In CGNs from *Gclm* (−/−) mice, initial responses to DomA (increase in intracellular calcium and L-glutamate release) are identical to those observed in GCNs from wild-type animals. Likewise, GSH efflux and a decrease of GSH levels upon DomA stimulation are also observed. However, because these latter effects cause a further reduction in GSH from an already low basal, ROS levels are higher and promote higher lipid peroxidation and enhanced toxicity in Gclm (−/−) CGNs.

These findings show that by activating AMPA/KA receptors (directly) and NMDA receptors (indirectly), the extent of DomA-induced neuronal death is dictated by intracellular GSH levels. DomA-induced oxidative stress is significantly more pronounced in *Gclm* (−/−) neurons, which have very low GSH levels. Thus, low levels of GSH, due either to genetic manipulation and/or to DomA-induced GSH efflux, may mediate DomA-induced neuronal cell death. Indeed, GSH depletion has been shown to cause mitochondrial dysfunction and activation of 12-lipoxygenase, resulting in the production of peroxides and the activation of neuronal magnesium-dependent sphingomyelinase and the production of ceramide (Liu et al., 1997). DomA-induced GSH efflux precedes any permeability of the cell membrane and may be explained by induction of a specific GSH transporter, such as seen with NMDA (Wallin et al., 1999). However, the exact mechanism of DomA-induced GSH efflux still needs to be investigated.

Additional evidence that GSH levels play a central role in modulating DomA toxicity is that depletion of GSH by BSO rendered CGNs from *Gclm* (+/+) mice as sensitive as CGNs from *Gclm* (−/−) mice. Conversely, increasing GSH levels in

TABLE 1

DomA-induced lipid peroxidation in CGNs

CGNs of both genotypes were exposed to 10 μ Μ DomA, alone or in combination with the indicated compounds and incubated at 37°C for 60 min. After 1-h recovery in maintenance growth medium, lipid peroxidation was assessed by the MDA assay. Results represent the mean ± S.D. of at least three experiments.

	MDA	
	Gclm (+/+)	*Gclm* (−/−)
	arbitrary units/μg protein	
Control	52 ± 7.0	91 ± 18.4*
DomA 10 μM	126 ± 12.7*	231 ± 20.5**
DomA + NBQX 10 μM	72 ± 8.2	113 ± 6.0
DomA + MK801 5 μM	79 ± 11.6	129 ± 5.1
DomA + GSHEE 2.5 mM	66 ± 14.1	94 ± 21.5

* Significantly different from untreated *Gclm* (+/+) neurons ($p < 0.05$)
** Significantly different from untreated *Gclm* (−/−) neurons ($p < 0.01$).

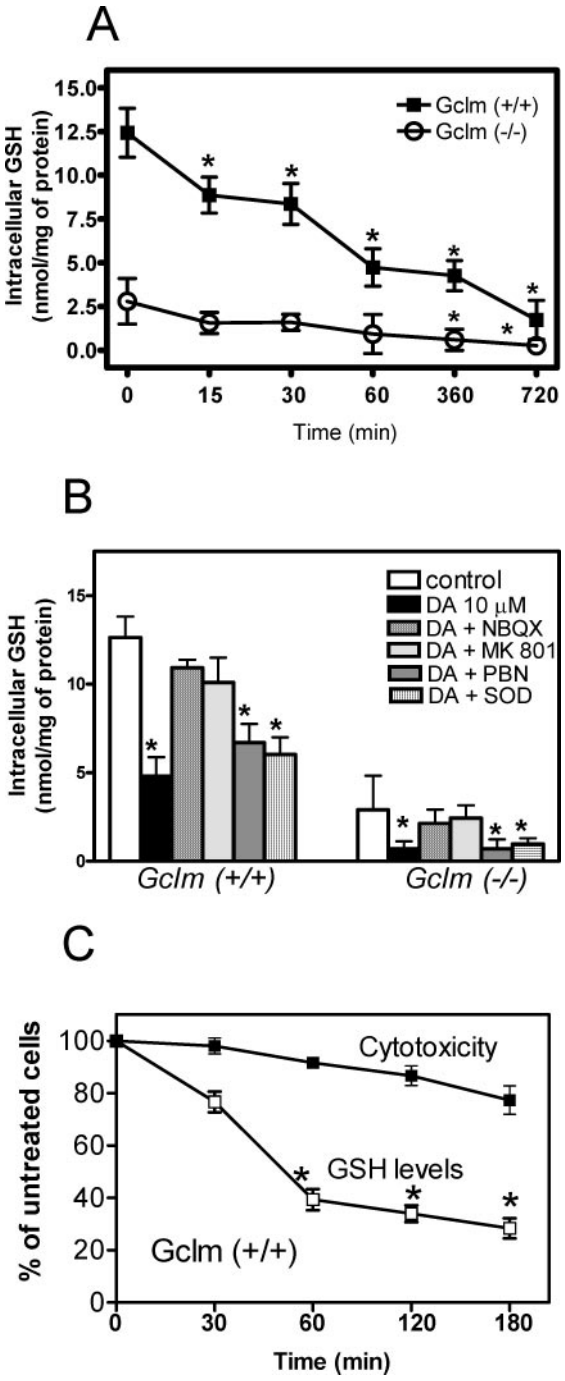

Fig. 8. A, time course of DomA-induced decrease of cellular GSH in CGNs. Results represent the mean ± S.D. of at least three experiments. *, significantly different from the respective control ($p < 0.01$). B, effect of 10 μM NBQX, 5 μM MK-801, 100 μM PBN, and 100 U/ml SOD on 10 μM DomA-induced GSH decrease in CGNs. Results represent the mean ± S.D. of at least three experiments. *, significantly different from control CGNs ($p < 0.01$). C, time course of 10 μM DomA-induced cytotoxicity (MTT assay) and decrease in intracellular GSH levels in CGNs from *Gclm* (+/+) mice. Result represent the mean ± S.D. of at least three experiments. *, significantly different from control ($p < 0.01$).

Gclm (−/−) neurons by means of GSHEE administration rendered them as resistant as their wild-type counterparts. This finding differs from that reported in mouse fibroblasts exposed to H_2O_2 (Yang et al., 2002). In that case, depletion of GSH with the glutathione transferase substrate phorone increased the sensitivity of *Gclm* (+/+) cells to H_2O_2 but not to the extent observed in *Gclm* (−/−) fibroblasts. Conversely, GSHEE afforded only partial protection against H_2O_2 in *Gclm* (−/−) cells. It was suggested that it is not the level of GSH itself, but the GSH synthetic potential, that may be the major determinant for protecting against oxidative insult (Yang et al., 2002). The different cell type, the use of BSO instead of phorone, and the ability of DomA to induce GSH efflux may be reasons for the observed differences between our results and those of Yang et al. (2002).

A relatively common C588T polymorphism has been discovered in the 5′-flanking region of the *GCLM* gene (Nakamura et al., 2002). Individuals carrying the T allele have lower promoter activity in a luciferase reporter gene assay in response to oxidants and significantly lower plasma GSH levels (Nakamura et al., 2002). These individuals are also at higher risk for myocardial infarction and present impairments in nitric oxide-mediated coronary vasomotor function (Nakamura et al., 2002, 2003). It would be interesting to know whether individuals carrying the T allele may also display lower GSH levels in the central nervous system and thus may be more susceptible to DomA-induced neurotoxicity. Evidence suggests that nonhuman primates may be more sensitive than rodents to DomA-induced neurotoxicity, and neonatal animals may be more susceptible than adults (Jeffery et al., 2004). Our results suggest that individuals with *GCLM* polymorphisms, or other mutations leading to decreased GSH levels (Dalton et al., 2004), would display an even enhanced sensitivity to DomA neurotoxicity.

An additional interesting finding of our studies relates to the effects of DomA in cerebellar astrocytes. The presence of ionotropic glutamate receptors in astrocytes is still the subject of debate (Seifert and Steinhauser, 2001). Clear evidence for a functional expression of KA receptors in astrocytes is lacking. However, electrophysiological and biochemical re-

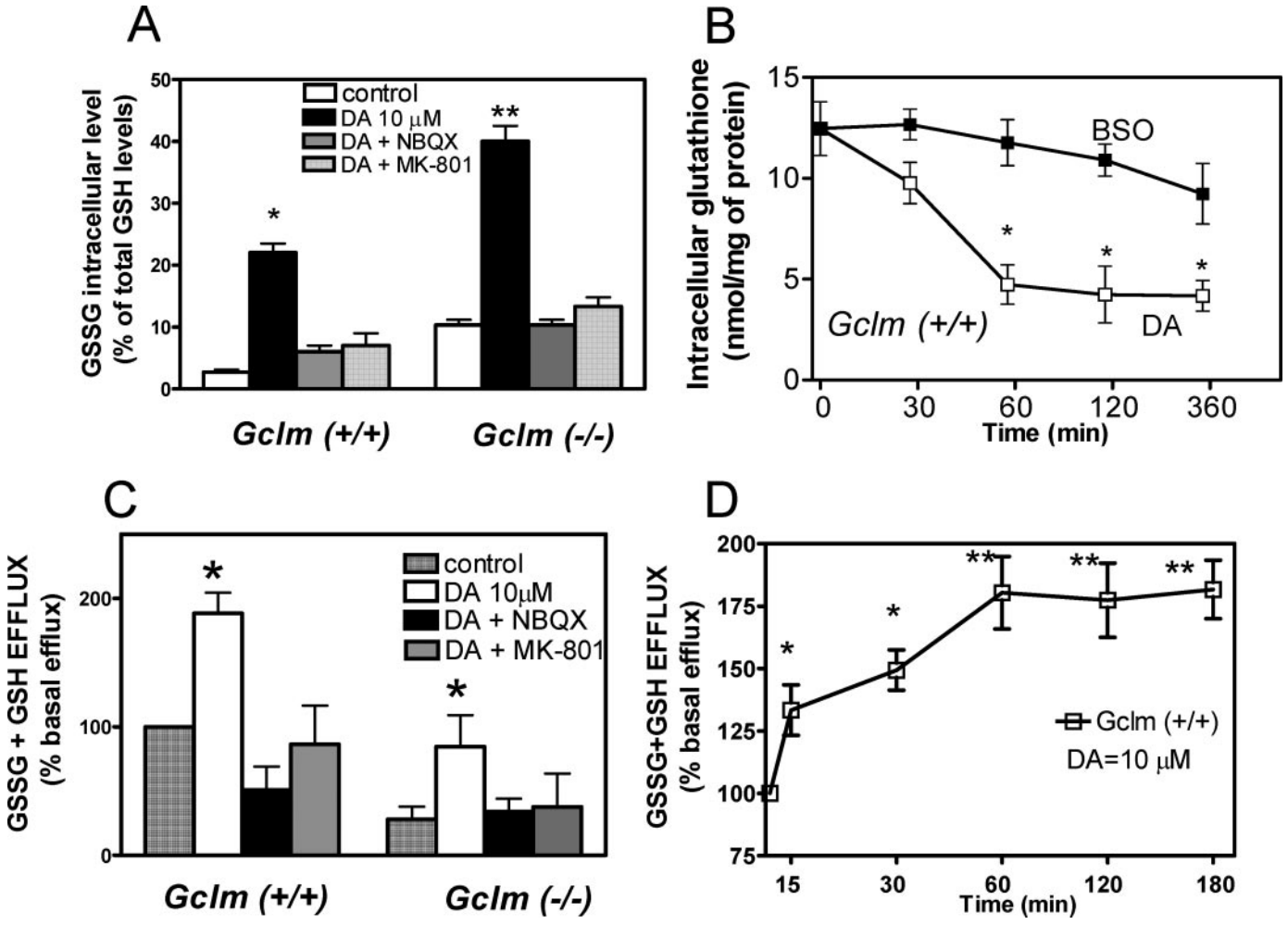

Fig. 9. A, effect of 10 μM DomA for 1 h, alone or in combination with 10 μM NBQX or 5 μM MK-801, on intracellular GSSG levels in CGNs. GSSG is expressed as percentage of total glutathione (GSH + GSSG). *, significantly different from control ($p < 0.01$). **, significantly different from control ($p < 0.005$). B, time course of GSH loss after treatment with 25 μM BSO or 10 μM DomA in *Gclm* (+/+) CGNs. Total glutathione content was assessed by the naphthalene dicarboxaldehyde assay. *, significantly different from control ($p < 0.05$). C, effect of 10 μM DomA for 1 h, alone or in combination with 10 μM NBQX or 5 μM MK-801, on GSH efflux in CGNs. Results are expressed as percentage of efflux of GSH present in untreated *Gclm* (+/+) CGNs. *, significantly different from the respective control ($p < 0.005$). D, time course of 10 μM DomA-induced GSH efflux in *Gclm* (+/+) CGNs. Results are expressed as percentage of efflux of GSH present in untreated *Gclm* (+/+) CGNs. *, significantly different from control ($p < 0.05$). **, significantly different from control ($p < 0.01$).

sponses to KA have been reported, possibly mediated by AMPA receptors (Telgkamp et al., 1996; Fan et al., 1999). Furthermore, whether NMDA receptors exist in astrocytes is also controversial (Ziak et al., 1998; Seifert and Steinhauser, 2001).

Our results clearly indicate that cerebellar astrocytes are resistant to DomA toxicity, and this holds true even for astrocytes from *Gclm* (−/−) mice, which have very low levels of GSH. Incubation of astrocytes with DomA elicited a modest increase in $[Ca^{2+}]_i$ compared with that observed in CGNs, and the response did not differ between the two genotypes. This small increase in $[Ca^{2+}]_i$ was due only to activation of AMPA/KA receptors, but it was not sufficient to elicit L-glutamate release and possible ensuing activation of NMDA receptors. The lack of a robust calcium response in astrocytes would explain their resistance to DomA toxicity, even in the presence of low GSH. Furthermore, no release of L-glutamate was observed in astrocytes in response to DomA. This finding would also support the suggestion that activation of NMDA receptors by AMPA/KA receptor-mediated stimulation of glutamate release is the initial more relevant step in DomA neurotoxicity (Berman et al., 2002).

Acknowledgments

The excellent technical assistance of Greg Martin (Keck Center, University of Washington, Seattle, WA) is gratefully acknowledged.

References

Ananth C, Gopalakrishnakone P, and Kaur C (2003) Protective role of melatonin in domoic acid-induced neuronal damage in the hippocampus of adult rats. *Hippocampus* **13:**375–387.
Berman FW, LePage KT, and Murray TF (2002) Domoic acid neurotoxicity in cultured cerebellar granule neurons is controlled preferentially by the NMDA receptor Ca^{2+} influx pathway. *Brain Res* **924:**20–29.
Berman FW and Murray TF (1997) Domoic acid neurotoxicity in cultured cerebellar granule neurons is mediated predominantly by NMDA receptors that are activated as a consequence of excitatory amino acid release. *J Neurochem* **69:**693–703.
Bondy SC and Lee DK (1993) Oxidative stress induced by glutamate receptor agonists. *Brain Res* **610:**229–233.
Bose R, Schnell CL, Pinsky C, and Zitko V (1992) Effects of excitotoxins on free radicals indices in mouse brain. *Toxicol Lett* **60:**211–219.
Carriedo SG, Yin HZ, Sensi SL, and Weiss JH (1998) Rapid Ca^{2+} entry through Ca^{2+}-permeable AMPA/kainate channels triggers marked intracellular Ca^{2+} rises and consequent oxygen radical production. *J Neurosci* **18:**7727–7738.
Ceccon M, Giusti P, Facci L, Borin G, Imbesi M, Floreani M, and Skaper SD (2000) Intracellular glutathione levels determine cerebellar granule neuron sensitivity to excitotoxic injury by kainic acid. *Brain Res* **17:**83–89.
Cheng Y and Sun AY (1994) Oxidative mechanisms involved in kainate-induced cytotoxicity in cortical neurons. *Neurochem Res* **19:**1557–1564.
Coyle JT and Puttfarcken P (1993) Oxidative stress, glutamate, and neurodegenerative disorders. *Science (Wash DC)* **262:**689–695.
Dalton TP, Chen Y, Schneider SN, Nebert DW, and Shertzer HG (2004) Genetically altered mice to evaluate glutathione homeostasis in health and disease. *Free Radic Biol Med* **37:**1511–1526.
Dutrait N, Culcasi M, Cazevieille C, Pietri S, Tordo P, Bonne C, and Muller A (1995) Calcium-dependent free radical generation in cultured retinal neurons injured by kainate. *Neurosci Lett* **198:**13–16.
Fan D, Grooms SY, Araneda RC, Johnson AB, Dobrenis K, Kessler JA, and Zukin RS (1999) AMPA receptor protein expression and function in astrocytes cultured from hippocampus. *J Neurosci Res* **57:**557–571.
Giordano G, Sanchez-Perez AM, Burgal M, Montoliu C, Costa LG, and Felipo V (2005) Chronic exposure to ammonia induces isoform-selective alterations in the intracellular distribution and NMDA receptor-mediated translocation of protein kinase C in cerebellar neurons in culture. *J Neurochem* **9:**143–157.
Guizzetti M, Bordi F, Dieguez-Acuna FJ, Vitalone A, Madia F, Woods JS, and Costa LG (2003) Nuclear factor kappaB activation by muscarinic receptors in astroglial cells: effect of ethanol. *Neuroscience* **120:**941–950.
Hampson DR and Manalo JL (1998) The activation of glutamate receptors by kainic acid and domoic acid. *Nat Toxins* **6:**153–158.
Huang J and Philbert MA (1995) Distribution of glutathione and glutathione-related enzyme systems in mitochondria and cytosol of cultured cerebellar astrocytes and granule cells. *Brain Res* **22:**16–22.
Jeffery B, Barlow T, Moizer K, Paul S, and Boyle C (2004) Amnesic shellfish poison. *Food Chem Toxicol* **42:**545–557.
Kooy NW, Royall JA, and Ischiropoulos H (1997) Oxidation of 2′,7′-dichlorofluorescein by peroxynitrite. *Free Radic Res* **27:**245–254.
Liang LP, Ho YS, and Patel M (2000) Mitochondrial superoxide production in kainate-induced hippocampal damage. *Neuroscience* **101:**563–570.
Liu B, Obeid LM, and Hannun YA (1997) Sphingomyelinases in cell regulation. *Semin Cell Dev Biol* **8:**311–322.
Lowndes HE, Beiswanger CM, Philbert MA, and Reuhl KR (1994) Substrates for neural metabolism of xenobiotics in adult and developing brain. *Neurotoxicology* **15:**61–73.
Miyamoto M and Coyle JT (1990) Idebenone attenuates neuronal degeneration induced by intrastriatal injection of excitotoxins. *Exp Neurol* **108:**38–45.
Nakamura S, Kugiyama K, Sugiyama S, Miyamoto S, Koide S, Fukushima H, Honda O, Yoshimura M, and Ogawa H (2002) Polymorphism in the 5′-flanking region of human glutamate-cysteine ligase modifier subunit gene is associated with myocardial infarction. *Circulation* **105:**2968–2973.
Nakamura S, Sugiyama S, Fujioka D, Kawabata K, Ogawa H, and Kugiyama K (2003) Polymorphism in glutamate-cysteine ligase modifier subunit gene is associated with impairment of nitric oxide-mediated coronary vasomotor function. *Circulation* **108:**1425–1427.
Oyama Y, Hayashi A, Ueha T, and Maekawa K (1994) Characterization of 2′,7′-dichlorofluorescein fluorescence in dissociated mammalian brain neurons: estimation on intracellular content of hydrogen peroxide. *Brain Res* **635:**113–117.
Perl TM, Bedard L, Kosatsky T, Hockin JC, Todd EC, and Remis RS (1990) An outbreak of toxic encephalopathy caused by eating mussels contaminated with domoic acid. *N Engl J Med* **322:**1775–1780.
Puttfarcken PS, Getz RL, and Coyle JT (1993) Kainic acid-induced lipid peroxidation: protection with butylated hydroxytoluene and U78517F in primary cultures of cerebellar granule cells. *Brain Res* **624:**223–232.
Scallet AC, Binienda Z, Caputo FA, Hall S, Paule MG, Rountree RL, Schmued L, Sobotka T, and Slikker W Jr (1993) Domoic acid-treated cynomolgus monkeys (*M. fascicularis*): effects of dose on hippocampal neuronal and terminal degeneration. *Brain Res* **627:**307–313.
Seifert G and Steinhauser C (2001) Ionotropic glutamate receptors in astrocytes. *Prog Brain Res* **132:**287–299.
Sheardown MJ, Nielsen EO, Hansen AJ, Jacobsen P, and Honore T (1990) 2,3-Dihydroxy-6-nitro-7-sulfamoyl-benzo(F) quinoxaline: a neuroprotectant for cerebral ischemia. *Science (Wash DC)* **247:**571–574.
Sobotka TJ, Brown R, Quander DY, Jackson R, Smith M, Long SA, Barton CN, Rountree RL, Hall S, Eilers P, et al. (1996) Domoic acid: neurobehavioral and neurohistological effects of low-dose exposure in adult rats. *Neurotoxicol Teratol* **18:**659–670.
Stewart GR, Zorumski CF, Price MT, and Olney JW (1990) Domoic acid: a dementia-inducing excitotoxic food poison with kainic acid receptor specificity. *Exp Neurol* **110:**127–138.
Strain SM and Tasker RA (1991) Hippocampal damage produced by systemic injections of domoic acid in mice. *Neuroscience* **44:**343–352.
Sun AY, Cheng Y, Bu Q, and Oldfield F (1992) The biochemical mechanisms of the excitotoxicity of kainic acid. Free radical formation. *Mol Chem Neuropathol* **17:**51–63.
Teitelbaum JS, Zatorre RJ, Carpenter S, Gendron D, Evans AC, Gjedde A, and Cashman NR (1990) Neurologic sequelae of domoic acid intoxication due to the ingestion of contaminated mussels. *N Engl J Med* **322:**1781–1787.
Telgkamp P, Backus KH, and Deitmer JW (1996) Blockade of AMPA receptors by nickel in cultured rat astrocytes. *Glia* **16:**140–146.
Thompson SA, White CC, Krejsa CM, Eaton DL, and Kavanagh TJ (2000) Modulation of glutathione and glutamate-L-cysteine ligase by methylmercury during mouse development. *Toxicol Sci* **57:**141–146.
Tryphonas L, Truelove J, Todd E, Nera E, and Iverson F (1990) Experimental oral toxicity of domoic acid in cynomolgus monkeys (*Macaca fascicularis*) and rats. Preliminary investigations. *Food Chem Toxicol* **28:**707–715.
Wallin C, Weber SG, and Sandberg M (1999) Glutathione efflux induced by NMDA and kainate: implications in neurotoxicity? *J Neurochem* **73:**1566–1572.
Wang H, Cheng E, Brooke S, Chang P, and Sapolsky R (2003) Over-expression of antioxidant enzymes protects cultured hippocampal and cortical neurons from necrotic insults. *J Neurochem* **87:**1527–1534.
White CC, Krejsa CM, DL Eaton, and Kavanagh TJ (1999) HPLC-based assay for enzyme of glutathione biosynthesis. *Curr Protoc Toxicol* 6.5.1–6.5.14.
Yang Y, Dieter MZ, Chen Y, Shertzer HG, Nebert DW, and Dalton TP (2002) Initial characterization of the glutamate-cysteine ligase modifier subunit *Gclm*(−/−) knockout mouse. Novel model system for a severely compromised oxidative stress response. *J Biol Chem* **277:**49446–49452.
Ziak D, Chvatal A, and Sykova E (1998) Glutamate-, kainate- and NMDA-evoked membrane currents in identified glial cells in rat spinal cord slice. *Physiol Res* **47:**365–375.

Address correspondence to: Dr. Lucio G. Costa, Department of Environmental and Occupational Health Sciences, University of Washington, 4225 Roosevelt Way NE, Suite 100, Seattle, WA 98105. E-mail: lgcosta@u.washington.edu